



# Monte Carlo studies of the COMPASS RICH 1 optical properties

G. Baum<sup>a</sup>, R. Birsa<sup>b</sup>, F. Bradamante<sup>b</sup>, A. Bressan<sup>b,1</sup>, A. Colavita<sup>c</sup>, S. Costa<sup>d</sup>, S. Dalla Torre<sup>b,\*</sup>, P. Fauland<sup>a</sup>, M. Finger<sup>e,f</sup>, F. Fratnik<sup>c</sup>, M. Giorgi<sup>b</sup>, B. Gobbo<sup>b,2</sup>, A. Grasso<sup>d</sup>, M. Lamanna<sup>b,2</sup>, A. Martin<sup>b</sup>, G. Menon<sup>b</sup>, D. Panzieri<sup>d</sup>, P. Schiavon<sup>b</sup>, F. Tessarotto<sup>b</sup>, A.M. Zanetti<sup>b</sup>

<sup>a</sup>University of Bielefeld, 33501 Bielefeld, Germany

<sup>b</sup>INFN, Sezione di Trieste and University of Trieste, Trieste, Italy

<sup>c</sup>INFN, Sezione di Trieste and ICTP, Trieste, Italy

<sup>d</sup>INFN, Sezione di Torino and University of Torino, Torino, Italy

<sup>e</sup>Charles University, Prague, Czech Republic

<sup>f</sup>JINR, Dubna, Russia

---

## Abstract

A dedicated Monte Carlo has been built to study the optical properties of the RICH 1 detector presently under construction for the COMPASS experiment at CERN. In this paper we focus on the optimization of the position of the photon detector with respect to the RICH mirror and on the alignment of the mirror elements forming the mirror surface. © 1999 Elsevier Science B.V. All rights reserved.

---

## 1. Introduction

COMPASS [1] is a fixed target experiment at CERN SPS designed to perform third generation polarized deep inelastic scattering measurements (semi-inclusive and inclusive measurements) and hadron spectroscopy studies. The set-up consists of two magnetic spectrometers (a large angle and a small angle spectrometer), each equipped with a hadron and an electromagnetic calorimeter, a muon filter and a RICH.

RICH 1 [2], which is a part of the first spectrometer, is presently under construction. It is a large acceptance gas RICH with 3 m long C<sub>4</sub>F<sub>10</sub> radiator at atmospheric pressure and at constant and uniform temperature. The mirror set-up consists of spherical mirrors, radius 6.6 m, segmented in 120 hexagonal pieces covering a total area larger than 20 m<sup>2</sup>, forming two spherical surfaces with different centres of curvature so as to focus the Cherenkov photons onto two sets of photon detectors placed above and below the acceptance region. The photon detectors are MWPCs equipped with CsI photocathodes covering a total active surface of 5.3 m<sup>2</sup> (see Fig. 1).

RICH 1 design has been achieved with the help of a dedicated Monte Carlo (reading GEANT [3])

---

\* Corresponding author.

<sup>1</sup> Presently Fellow at CERN.

<sup>2</sup> Presently Research Associate at CERN.

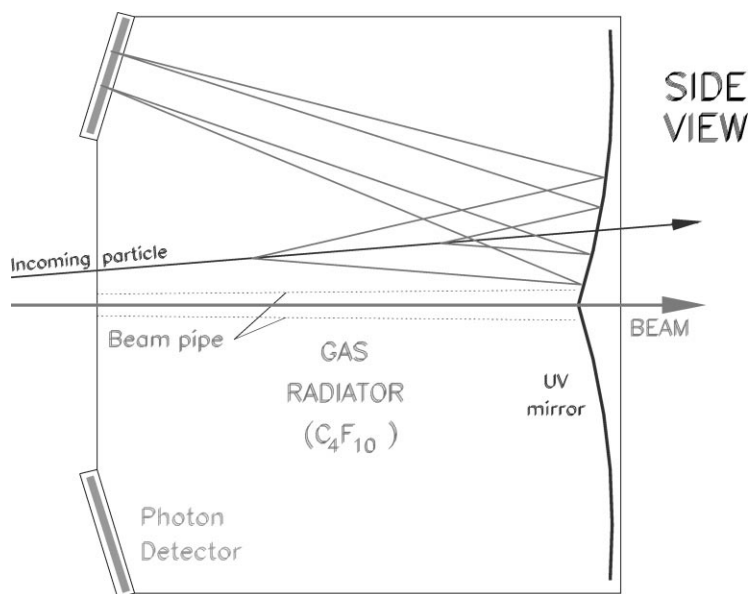


Fig. 1. The schematic side view of the RICH showing the relative positions of the mirrors, the photon detectors, the beam line and some typical photon trajectories.

generated data files), built to study the optical properties of the detector [4–8]. In this paper we report on the optimization of the position of the photon detector with respect to the RICH mirror and on the alignment of the mirror elements forming the mirror surface.

## 2. Optimization of the detector position by MC simulation

The formation of the *ring* image can be understood as follows: the photons emitted at fixed angle  $\theta$  around the particle trajectory ‘focus’ at space points that form a closed curve on the detector surface. The resulting image can be approximated by an ellipse with the orientation of its axes depending on the particle trajectory (see. e.g., Fig. 2).

The optimization of the detector position has been achieved by two methods.

In the simulation for method 1, particles are generated by means of GEANT (LEPTO [9] generator) for a realistic ‘illumination’ of the mirror; only one particle per event is used and the condition  $\beta = 1$  is forced. Cherenkov photons (typically

30) are emitted along the particle trajectory inside the radiator, at a constant Cherenkov emission angle  $\theta_C$ , with a uniform distribution in distance along the particle path and in angle  $\phi_C$  around the particle trajectory. Photons then reflect on the RICH mirror and hit the detector surface. Other effects which spoil the detector resolution (particle multiple scattering, effect of the residual magnetic field, mirror imperfections, chromatic dispersion) are not taken into account for this application. For each generated event (same particle and same related photons), the position of the flat detector is systematically varied on a grid of values of angle between the detector plane and the vertical axis ( $\theta_D$ ) and position along the nominal beam axis ( $z_D$ ), typically  $11 \times 9$  configurations. For each detector position, the value of  $\sigma_\theta^2$  (variance of the distribution of  $\Delta_\theta$ , average, for the Cherenkov photons of each particle, of the difference between the MC generated ( $\theta_C$ ) and the reconstructed ( $\theta_Y$ ) photon Cherenkov angle) is computed and plotted as a two-dimensional distribution. The detector configuration ( $\theta_D$ ,  $z_D$ ) corresponding to  $\sigma_\theta^2$  minimum can then be evaluated. The reconstruction method used is from the literature (see, e.g., [10]); the spread

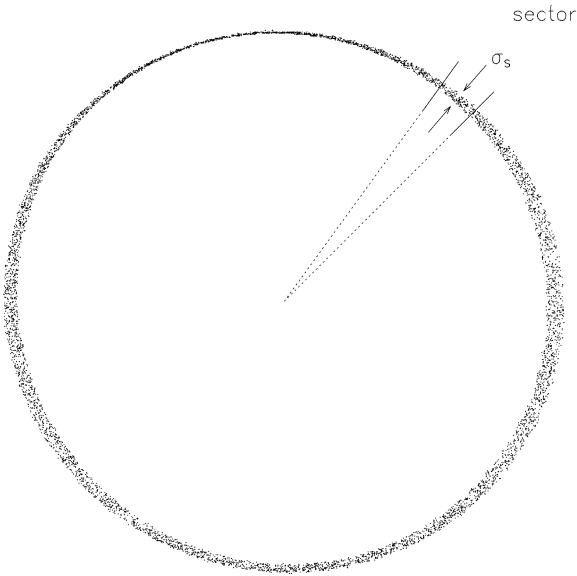


Fig. 2. Example of distribution on the detector surface of the impact points of the Cherenkov photons emitted by a  $\beta = 1$  particle (at angles  $\theta_p = 8^\circ$  and  $\phi_p = 45^\circ$  with respect to the beam axis) and reflected on the RICH mirror; the relative width of the *ring* has been magnified by a factor of 10 for presentation. One of the 40 angular sectors is also shown.

of  $\Delta_\theta$  is due to the spherical aberrations introduced by the uncertainty in the photon emission point; typical values of  $\sigma_\theta$  at the minimum are 0.1 mrad.

For method 2, particles and photon trajectories are generated as for the studies with method 1. The typical number of generated photons for this approach is 10 000. The detector position is varied on a grid of position as described for the previous method. For each event (same particle and same related photons), the *ring* is divided into 40 sectors (each  $9^\circ$  wide); for all the photon hits in each sector, the distance from the approximate centre of the ring (*radius*) is calculated and then the mean quadratic difference, divided by the *radius* squared ( $\sigma_s^2$ ) (see Fig. 2) is computed;  $\sigma_r^2$ , the average value of  $\sigma_s^2$ , is then computed over all the sectors of the *ring* to avoid the dependence on the position of the centre.  $\sigma_r^2$  is some measure of the area covered by the photon hits. For each detector position the value of  $\langle \sigma_r^2 \rangle$  is computed, averaged over all the events generated ( $\langle \sigma_r^2 \rangle_{ev}$ ) and then plotted as a two-dimensional distribution, which exhibits an evident minimum.

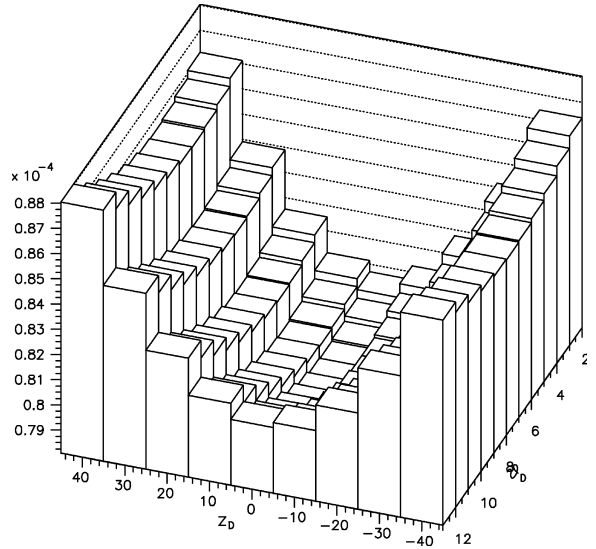


Fig. 3. Example of the distribution of the figure of merit as a function of the detector configuration  $\theta_D$ ,  $z_D$  obtained using method 1: the channel content is the square root of the variance of the reconstructed Cherenkov emission angle ( $\sigma_\theta^2$ ).

The minimum in the plane  $\theta_D$ ,  $z_D$  (see, e.g., Fig. 3) is rather wide but well defined using both methods and an optimized position of the detector can be obtained with both approaches and the results of the two methods are in good agreement.

There is an appreciable dependence of the minimum position on the particle sample used in the simulation: this feature should certainly be taken into account when tuning the detector position using these methods.

### 3. Studies of mirror characteristics by MC simulation: mirror element alignment

Each one of the upper and the lower mirror of the RICH is made by an array of as many as 60 spherical mirror elements, in principle all equal, put side by side to form a continuous spherical surface; to simplify the geometry of this simulation, the mirror elements have a square shape (400 mm  $\times$  400 mm) instead of the hexagonal shape foreseen. The mirror construction procedure will result, among other imperfections, in some spread of the

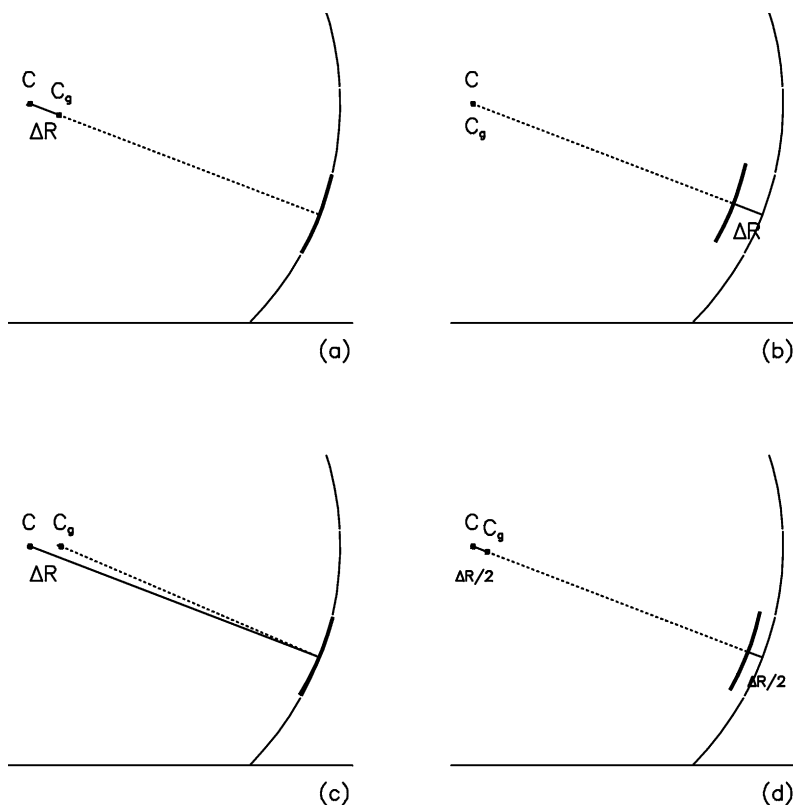


Fig. 4. Four possible methods of positioning the mirror elements are illustrated; in these examples, the radius is shorter than  $R_0$  by  $\Delta R$ ;  $C$  is the nominal centre position,  $C_g$  the actual one.

value of the radius of curvature  $R$  of the individual mirror pieces around the nominal value  $R_0$ ; let  $\Delta R$  be the difference. The question is how to put together the mirror elements to obtain the best reflecting surface, knowing  $\Delta R$  for each mirror element.

Fig. 4 shows four possible methods of positioning the mirror elements to get the mirror surface. In Fig. 4(a) the mirror element surface is on the nominal mirror surface, but the radius is shorter than  $R_0$  by  $\Delta R$ . In Fig. 4(b) the mirror element centre is kept in the nominal position and its surface moved toward the centre by  $\Delta R$ . In Fig. 4(c) the correction of the centre position is along the  $z$ -axis and the mirror element results slightly tilted. In Fig. 4(d) a possible intermediate solution between (a) and (b) is assumed.

Given a sample of mirror elements produced with a gaussian distribution of  $\Delta R$ , with standard

deviation  $\sigma_R$  of 33 mm (1% of  $R_0$ ), the mirror elements of different radii can be distributed over the mirror surface with different recipes; we have studied the following configurations: random distribution and mirror ordered in space according to radius value (*parabolic* and *anti-parabolic* distributions). In the simulation, photons (typically 30) are emitted by each of a suitable sample of particle and, after reflection and detection, the emission angle of each of them is reconstructed and compared with the MC value; the variance of this distribution ( $\sigma_\theta^2$ ) is then evaluated. Results are presented in Table 1.

These studies indicate that on keeping the mirror element on the nominal mirror surface, a clearly better result is obtained. A substantial improvement can be obtained sorting the mirror according to the radius value: we can divide the sample into two, taking, e.g., the larger radius mirror elements for the upper mirror surface and the smaller ones

Table 1  
Resolution  $\sigma_\theta$  in reconstructed Cherenkov angle  $\theta_C$  assuming  $\sigma_R = 33$  mm (1%)

Mirror element distribution	Alignment mode	$\sigma_\theta$ ( $\mu\text{rad}$ )
Random	(a)	184.
Random	(b)	470.
Random	(c)	202.
Random	(d)	430.
'Parabolic' corrected <sup>a</sup>	(a)	171.
'Anti-parab.' corrected <sup>a</sup>	(a)	163.
Spherical aberr. (for comparison, not included above)		95.

<sup>a</sup>Due to the particle distribution on the mirror surface, the mirror elements closest to the centre (beam line) are hit more frequently; the effective average value of  $\Delta R$  is then different from 0 and then the value of  $R$  used in the reconstruction is  $R_0$  'corrected' to take into account this effect

for the lower, with different average (nominal) values for upper and lower mirror sets, but smaller spread. There is no appreciable gain using 'parabolic' or 'anti-parabolic' shapes, but further improvement on the average resolution  $\sigma_\theta$  can be achieved as follows: given the RICH geometry, the spot due to the photons emitted by the same particle hit on the mirror surface a circular region (330 mm diameter for  $\beta = 1$ ), contained in, at most, three mirror elements of hexagonal shape; putting close to each other the mirror elements with similar radii and knowing the particle impact point on the mirror, we can use in the reconstruction the average value of the three radii (this correction is not included in the results presented in Table 1).

## 4. Conclusions

We have presented examples of studies of RICH 1 optical properties obtained by a dedicated Monte Carlo. This flexible tool has been widely employed to finalize the detector design and to understand the detector performances and the resolution in the measured Cherenkov angle.

## References

- [1] The COMPASS Collaboration, Common muon and proton apparatus for structure and spectroscopy, Proposal to the CERN SPSLC, CERN/SPSLC/96-14, SPSC/P 297, March 1, 1996; Addendum, CERN/SPSLC/96-30, SPSLC/P 297 Add. 1, May 20, 1996.
- [2] G. Baum et al., Nucl. Instr. and Meth. A 433 (1999) 207.
- [3] GEANT 3.21, CERN Program Library Long Writeup W5313, October 1994.
- [4] P. Schiavon, Studies of the effects of multiple Coulomb scattering and measuring errors on the Cherenkov emission angle reconstruction, COMPASS Internal Note, 7 October 1997; rev.: 23 October 1997, 26 November 1997.
- [5] P. Schiavon, Studies of the Cherenkov emission angle reconstruction. Part 1, COMPASS Internal Note, 10 June 1997; rev.: 7 November 1997.
- [6] P. Schiavon, Studies of the Cherenkov emission angle reconstruction. Part 2, COMPASS Internal Note, 27 June 1997; rev.: 27 November 1997.
- [7] P. Schiavon, Studies of the effect of the mirror radius value on the reconstruction of the Cherenkov angle by Monte Carlo simulation, COMPASS Internal Note, 14 May 1997; rev.: 17 December 1997.
- [8] P. Schiavon, Studies for the optimization of the RICH 1 detector position by Monte Carlo simulation, COMPASS Internal Note, May 1997; rev.: 5 January 1998.
- [9] G. Ingelman, LEPTO 6.3, 17 July, 1995.
- [10] T. Ypsilantis, J. Seguinot, Nucl. Instr. and Meth. A 343 (1994) 30.